Zeitschrift fuer Medizinische Physik xxx (xxxx) xxx

Contents lists available at ScienceDirect

Zeitschrift für Medizinische Physik

journal homepage: www.elsevier.com/locate/zemedi

Off beam dosimetry for risk group classification for patients with head and neck cancer and CIED

Larissa Blümlein [a,b,*], Oliver Kölbl [a], Ralf Ringler [b], Barbara Dobler [a]

[a] Department of Radiotherapy, University Hospital Regensburg, Germany
[b] OTH Amberg-Weiden, Technical University of Applied Sciences, Germany

ARTICLE INFO

Keywords:
Off-beam dosimetry
Cardiac implantable electronic devices
Risk management
Safe classification

ABSTRACT

Current guidelines [1] classify patients with cardiac implantable electronic devices (CIED) into risk groups based on the maximal CIED dose (D_{max}) to avoid malfunctions. If a CIED is located outside the radiation field, dose calculation by treatment planning systems (TPS) is not sufficiently accurate for safe classification. In certain cases, a magnet is placed on the CIED for deactivation of antitachyarrhythmia (ATA) therapy during treatment. The magnet is, however, not included in the treatment planning process, which leads to further uncertainty in the dose determination at the CIED. The aim of the study was to investigate the influence of the magnet on CIED dose and to examine if the inclusion of the magnet in the TPS allows a more accurate dose prediction for safe classification of the patients. Treatment plans with and without the magnet were calculated for 15 patients with naso-/orpharyngeal or esophageal carcinoma and transferred to a phantom with integrated CIED. Treatment plan verification was performed with thermoluminescence detectors (TLDs) and radiochromic films. Our study showed an overestimation of the dose in the CIED by the TPS by 0.4 Gy (20 %) on average. The magnet used for ATA deactivation during radiotherapy increased the dose to the CIED slightly by 0.1 Gy on average. For Volumetric Modulated Arc Therapy (VMAT) irradiations of patients with esophageal or oro-/nasopharyngeal carcinoma, placement of the magnet had no clinically relevant impact on the CIED dose in most of the cases. The inclusion of the magnet in the TPS had no influence on calculated CIED dose and did not change the classification into risk groups. Despite uncertainties in the dose calculation, risk classification by the TPS Monaco was safe in 97 % of the cases, even if a magnet was used for ATA deactivation and not included in the treatment planning process.

Introduction

Every year, there are around 75.500 new implantations of active medical implants such as pacemakers (PM) or implantable cardioverter defibrillators (ICD) in Germany. This number has remained constant over the recent years [2,3]. Independent of this, the patient group with newly occurring cancers is growing due to the overall increase in life expectancy. Modern diagnostic and therapeutic procedures used in cancer therapy involve the application of ionizing radiation. Ionizing radiation can trigger malfunctions in active implants such as pacemakers and defibrillators. Current guidelines [1,4,5] draw attention to the enormous importance of this topic: The risk is assigned according to the patient's dependence on the pacemaker or defibrillator and the distance of the implant from the tumor and the estimated dose at the implant. Table 1 gives an overview of the classification of the patient into the three risk groups "low", "medium" and "high". The American Association of Physicists in Medicine (AAPM) Report of the Task Group 203 "Management of Radiotherapy Patients with Implanted Cardiac Pacemakers and Defibrillators'' [4] also describes potential failure modes of PMs and ICDs and gives advice for patient management during the whole radiotherapy process. The dose at the implant is determined prior to irradiation by the treatment planning system (TPS). The dose calculation algorithms used in the TPS have proven to accurately predict the dose in the tumor and in proximal organs at risk. Whereas the calculation of other algorithms, such as the Analytical Anisotropic Algorithm (AAA), deviate strongly from dose measurements in the out-of-field region, in which the CIED is located, the X-ray Voxel Monte Carlo Algorithm (XVMC) used in this work shows higher agreement to measurements in this area. Nevertheless, there are deviations larger than 20 % between the dose calculation and the measurements in the out-of-

* Corresponding author at: Department of Radiotherapy, University Hospital Regensburg, Germany.
E-mail address: l.bluemlein@ukr.de (L. Blümlein).

https://doi.org/10.1016/j.zemedi.2025.08.001
Received 19 February 2025; Accepted 6 August 2025

0939-3889/© 2025 The Author(s). Published by Elsevier GmbH on behalf of DGMP, ÖGMP and SSRMP. This is an open access article under the CC BY license (http://creativecommons.org/licenses/by/4.0/).

Table 1
Risk group classification. Classification of patients into three different risk groups according to the DEGRO/DGK guideline [1]

	Dose < 2 Gy	Dose 2-10 Gy	Dose > 10 Gy
No pacemaker dependence	low	medium	high
Patient pacing dependent	medium	high	high

field, as shown in Mille et al. [6]. Therefore, measurements in the scattered radiation area are required to reliably classify patients into risk groups. In certain cases if the patient is pacing dependent, a magnet is placed on the CIED during treatment for deactivation of antitachyarrhythmia (ATA) therapy [7]. The common strength of the magnetic field is given in the literature as 9 mT [8]. The magnet is, however, not included in the treatment planning process. This may lead to further uncertainty in the CIED dose determination. The purpose of this study was to investigate the influence of the density of the magnet on CIED dose and to determine whether the inclusion of the shape and density of the magnet in the treatment planning process increases the accuracy of the dose prediction and the classification into risk groups for patients with esophageal or naso-oropharyngeal carcinoma. The magnetic field was not included in the investigation.

Methods

Phantom development

To determine the scattered radiation dose directly around the active implant an in-house Polymethylmethacrylate (PMMA) thoracic slab phantom was designed. PMMA has a density of 1.18 g/cm^3 and has equivalent interaction properties with ionizing radiation to those of human tissue. The radiation transport properties such as absorption and scattering are therefore very similar to those of soft tissue [9]. The phantom layers are drawn using design software CATIA (Dassault Systèmes, Vélizy-Villacoublay, France) and then manufactured. For dose measurements with thermoluminescence detectors (TLDs), small holes with a diameter of 1.2 mm and a depth of 7.0 mm, were drilled at a distance of 0.3 cm from the implant and at a distance of 1.5 cm to each other around the implant (Fig. 1a). The phantom is built of 1 cm slices and includes a CIED-Module embedded in wax (Fig. 1b). In order to cover not only tumors in the thoracic but also in the head and neck region, an adapter plate was developed to connect the head of the Alderson phantom to the thoracic phantom (Fig. 1c). Radiochromic films can be inserted between the slabs. A 3D printed dummy magnet was used to include the magnet in the treatment planning process (Fig. 1d). The dummy magnet was positioned on the phantom above the CIED and markers were attached to the phantom surface to reproduce the position of the magnet during treatment. Computed tomography (CT) images of the setup described above were acquired using a SOMATOM Sensation Open (Siemens Healthineers AG, Forchheim, Germany).

Patients and treatment planning

For 15 patients with oesophageal or naso- and oropharyngeal carcinoma, treatment planning was performed in the TPS Monaco (Elekta AB, Stockholm, Sweden) using different energies such as 6 MV and 6 MV flattening filter free (FFF) and Volumetric Modulated Arc Therapy (VMAT) techniques as partial dual- or triple arcs avoiding direct irradiation of the implant and magnet. Prescription for oesophageal carcinoma was 1.8 Gy per fraction to a total dose of 45.0 Gy and for naso-oropharyngeal carcinoma 2.0 Gy to 70.0 Gy. The maximum dose to the CIED should be as low as reasonably possible without compromising target dose. The XVMC algorithm (Elekta AB, Stockholm, Sweden) was used for dose calculation. After treatment planning all treatment plans were transferred to the CT scan of the phantom. The CT images were registered with respect to the CIED positions. In general, the distances between planning target volume (PTV) and CIED are variable in the treatment plans and differ between 3 - 10 cm. TLD positions in the phantom were contoured in the TPS as Regions of Interest (ROIs) for comparison of measured dose with calculated dose. The maximum dose over all TLD ROI was used as a surrogate of maximum dose in the CIED. Plans were then categorised into low, medium and high risk according to Table 1 assuming no pacemaker dependence.

The following two scenarios were simulated:

1. Treatment with a magnet: the 3D printed magnet was assigned a relative electron density of 6.6 equivalent to ferromagnetic iron.
2. Treatment without magnet: the 3D printed magnet was excluded from the external contour.

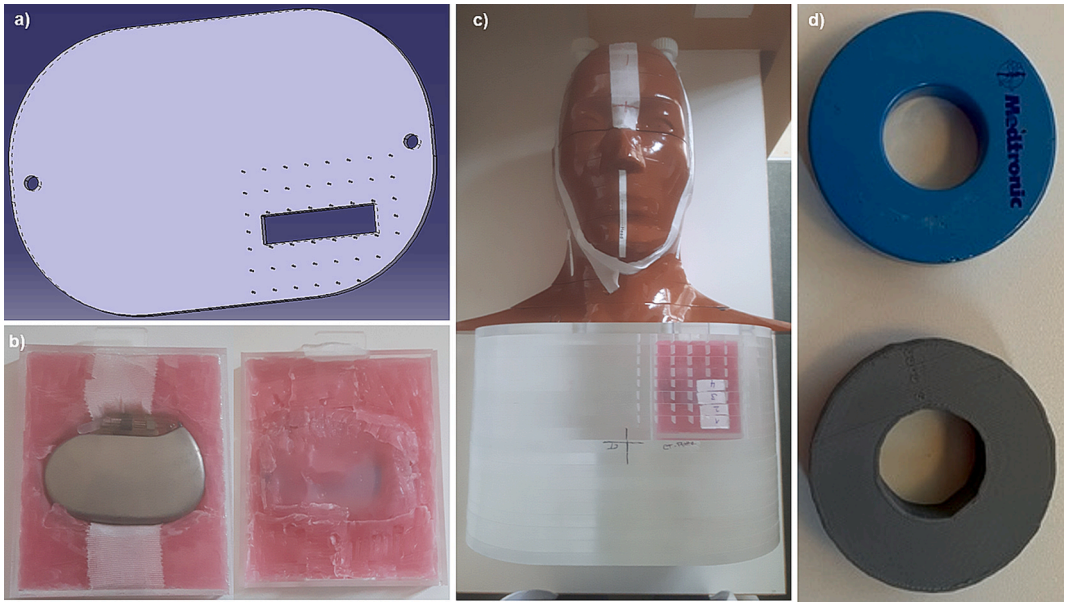


Fig. 1. Phantom. (a) Technical drawing of the phantom with TLD and CIED inserts, (b) CIED-Module embedded in wax, (c) Phantom with Alderson head connected to PMMA slab phantom, (d) Real magnet (upper part in blue) and corresponding 3D printed dummy magnet (lower part in grey).

TLD calibration and measurement

To cover a wide energy and dose range, two different kinds of lithium fluoride TLDs were used for dose measurements: LiF:Mg,Cu,P (MCP, RadPro International GmbH, Remscheid, Germany) and LiF:Mg,Ti (MTS, RadPro International GmbH, Remscheid, Germany) – both square rods with dimension of 6 mm x 1 mm x 1 mm. These TLDs are widely used in combination for out-of-field dosimetry due to the different energy dependence of the detector response [10]. MCPs tend to under response while MTS tend to slight over response at energies below 400 keV, the range in which the energy of the 6 MV out-of-field energy is assumed [11]. As mentioned in Hauri et al. [12] using a combination of tissue equivalent TLDs, both corrected measurements can be used to determine out-of-field dose and enabling a more precise result. For proper results, MCPs and MTS were combined and the mean of both measurements was calculated. The background was determined by two unexposed TLDs and the mean was subtracted from each raw measurement result. Since we used completely new TLDs, these were first stabilized by repeated irradiation and evaluation. The calibration factor and its relative deviation to the last calibration factor were determined several times for each TLD to observe the whole stabilization process. Calibration was performed in a solid water (RW3) slab phantom at a depth of 5 cm with 100 MU 6 MV photon beam, source to surface distance (SSD) 100 cm and a field size of 20 x 20 cm^2. Measurement with an ionisation chamber had previously been performed with the same parameters to determine the absolute dose. The TLD reader Harshaw QS 5500 (Thermo Fisher Scientific Inc., Massachusetts, USA) was used to read the TLDs. Post and pre-annealing were performed using the TLD Heat Annealing Oven (RadPro International GmbH, Remscheid, Germany). An uncertainty of 9 % resulted from the dose measurements using the relative difference of the last two calibrations. The average of the relative differences over all TLDs was calculated. The value was compared with measurement uncertainties in the out-of-field range (4–12 %) according to Kry et al. [13] and considered the measurement uncertainty in this study.

Radiochromic film calibration and measurement

Additional dose verification was carried out by means of radiochromic films (EBT3 Gafchromic™ radiotherapy films, Ashland Inc., Wilmington, USA) [14]. Films were cut into rectangular pieces for calibration and marked in relation to the original sheet to indicate their orientation for scanning. Calibration films were exposed with different dose levels covering the dose range of a fraction of each plan. As described in Menegotti et al. [15] and Maerz et al. [16], films were scanned 12 hours after irradiation at the earliest to account for the post-irradiation processing of the films. For the scan parameters, the same settings were used as described in [15,16]. All films were scanned with an EPSON Perfection V850 Pro Photo scanner (Seiko Epson Corporation, Suwa-shi, Japan) and converted to dose files with an in-house written MATLAB script (MathWorks Inc., Natick, USA). The dose evaluation was performed using the software MyQA (IBA Dosimetry GmbH, Schwarzenbruck, Germany). The uncertainty of dose measurements following this method was reported to be 2.0 % for MV-Beams [17,18].

Setup and measurement

In order to investigate the influence of direct irradiation of the magnet, a first measurement was made with a simplified setup. A RW3 slab phantom and radiochromic films were used for this purpose as shown in Fig. 2. An energy of 6 MV and a field size of 10 x 10 cm, SSD 100 cm and 2 Gy were used. The magnet was partially placed in the radiation field to investigate the influence of the magnet on the dose to the skin (Fig. 2a). Furthermore, five radiochromic films were placed in different depths: one film at the surface and the other four at depths of 1 cm to 4 cm below the magnet (Fig. 2b). A reference measurement without magnet was carried out. The scanned films were analysed using the software MyQA. The reference measurement was compared with the measurement with magnet and the mean dose within one ROI was determined at different depths and at the phantom surface.

For the main investigation with the thoracic phantom for clinical cases a cone-beam CT (CBCT) was acquired to position the phantom and mark the isocentre on phantom surface for each treatment. After that, TLDs and films were placed in their measurement position. Subsequently, 2 × 8 TLDs are placed around the CIED in two phantom layers. In order to generate as little deviation from the dose calculation in the TPS as possible. The absorption and backscatter effects of the implant should also be included in the measurements. Therefore, the TLDs and films were placed around the implant in the pre-defined holes in the phantom and not instead of the CIED as shown in Fig. 3. Two radiochromic films are placed around the CIED insertion module and on the TLDs, too. The position of the TLDs is then marked on the films so that a comparison between film and TLD measurements is possible afterwards. This ensures reproducibility of the measurements at the same points. Each treatment plan was measured twice – first with MCP and films and second with MTS and films. All measurements were performed with and without the real magnet on the phantom surface.

Statistical evaluation

The required number of patients was determined according to Cohen [19]. The probability of Type I, or α, error should be smaller than 0.05 and that of a Type II, or β, error, smaller than 0.2. Case number analysis using the software GPower3.1 (Heinrich Heine Universität, Düsseldorf, Germany) [20,21] resulted in a sample size of 11 patients. Due to the condition that all the patients must also be carriers of an implant, the

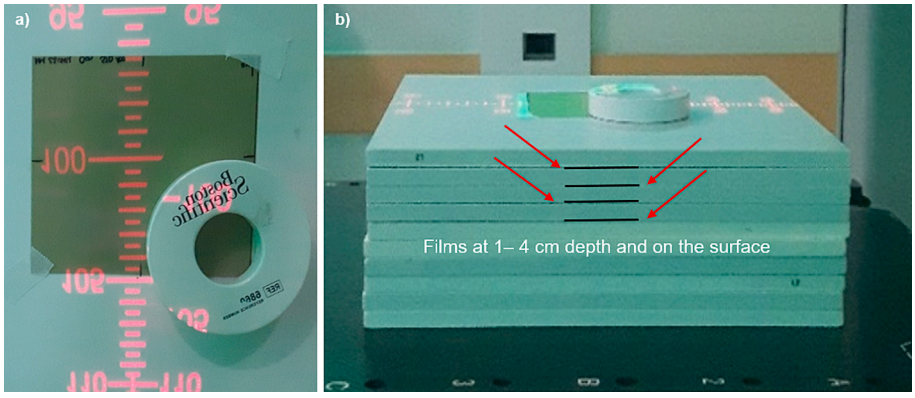


Fig. 2. Direct irradiation of the magnet in the RW3 slab phantom. a) Radiographic film measurement on the surface directly below the magnet, b) Measurement positions of the films at a depth of 1 cm to 4 cm below the magnet.

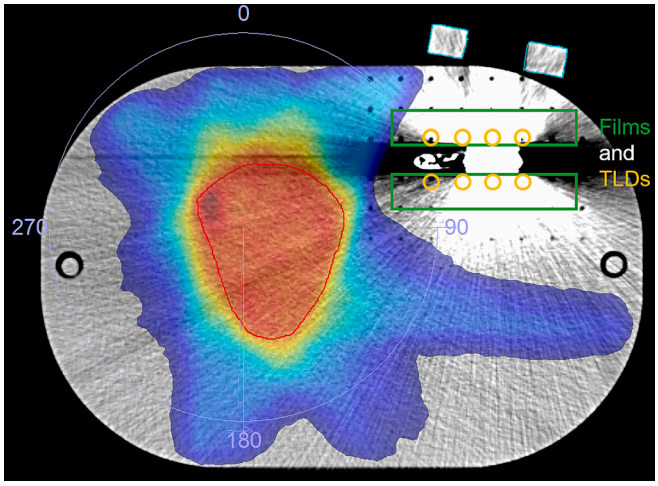


Fig. 3. Treatment planning and measurement setup with films and TLDs. Transverse section through the phantom with dummy magnet on surface. TLD (yellow ROIs) and film positions (green ROIs) are marked as an example.

number of patients for the tumour entity of naso-oropharyngeal carcinoma could not be reached. To ensure statistical significance of the results, both entities were combined for statistical analysis, leading to a final number of 15 patient plans included in the statistical evaluation. Due to the different dose prescriptions, we calculated and analysed the dose differences for the descriptive statistical analysis and did not use the measured or calculated raw values at each point. This approach means that the difference due to the dose prescriptions has no influence on the actual result. In summary, 240 measurement and calculation points were evaluated for each of the following comparisons.

The following comparisons were performed:

1. Quantification of deviations between measurement methods:
   - Comparison of TLD to film measurements, both without magnet
2. Quantification of deviations between off-beam dosimetry and TPS:
   - Comparison of measurements (TLD and film) to calculation, all without magnet
3. Quantification of actual influence of the magnet on the dose to the CIED:
   - Comparison of TLD measurements with magnet to without magnet
   - Comparison of film measurements with magnet to without magnet
4. Quantification of the influence of the virtual magnet on the calculated dose distribution
   - Comparison of TPS calculations without and with magnet
5. Assessment of actual clinical workflow
   - Comparison of TLD and film measurements with magnet to TPS calculation without magnet
6. Assessment of adapted clinical workflow
   - Comparison of TLD and film measurements with magnet to TPS calculation with magnet
7. Assessment of classification into risk groups
   - Comparison of classification according to TPS calculation and measurements

Absolute dose differences were calculated for descriptive statistical analysis with mean and 95 % confidence interval (95 %-CI). The confidence interval was determined using the bootstrap method [22]. For statistical analysis of the measurement data, Wilcoxon signed rank test with a significance level of p-value < 0.05 was used to detect relevant differences. The software SPSS Statistics (IBM, New York, USA) was used for this purpose.

Results

Direct irradiation of the magnet in the first simplified measurement setup in the RW3 slab phantom showed a skin dose increased by a factor of 5 as compared to the irradiation without magnet. Dose profiles of the film measurements on the phantom surface with and without magnet are given in Fig. 4. Maximum surface doses were 1.9 Gy for irradiation with magnet (yellow line) and 0.4 Gy without magnet (green line). Furthermore, the results in the RW3 slab phantom showed relative dose differences below the magnet of 20 % at depths of 3 cm and 4 cm and 21 % at a depth of 5 cm. This represents an absolute dose difference of 0.4 Gy at a depth of 3 cm for a single 2.0 Gy fraction as compared to the reference measurement without the magnet. These are the depths in which the CIED and detectors were located in the second setup.

The results of the CIED-phantom study are described below and summarized in Table 2. Fig. 5 shows boxplots of the absolute dose differences. As for standard boxplots, the red marker in the middle shows the median. The lower and upper edges show the 1st and 3rd quartiles while the black whiskers show the extreme data points up to 3 interquartile ranges. The red symbol "+" demonstrates outliers larger than 3 interquartile ranges. The p-value is shown in each figure.

Direct comparison between TLD and film measurements without magnet is shown in the boxplot in Fig. 5a. The comparison resulted in an absolute mean dose difference of -0.1 Gy with a 95 %-CI of [-0.6 Gy; 0.8 Gy] corresponding to a relative mean dose difference of -3 %. Negative values represent film doses larger than TLD doses. The differences were significant in all cases with $p < 0.001$ in the Wilcoxon signed rank analysis.

Film and TLD measurements without and calculation without magnet resulted in the following means of dose differences (Fig. 5b): −0.4 Gy and a 95 %-CI of [−1.5 Gy; 0.3 Gy] for comparison of TLDs and TPS and −0.4 Gy with a 95 %-CI [−1.4 Gy; 0.4 Gy] for films and TPS. This corresponds to mean relative dose differences of −20 % for TLDs and TPS and −20 % for films and TPS. Negative values represent calculated doses larger than measured doses. The Wilcoxon signed rank test showed significant differences with $p < 0.001$.

Fig. 5c shows the results of dose deviations between measurements without and with magnet. The quantification of the actual influence of the magnet on the dose to the CIED resulted in a mean dose difference of −0.1 Gy for TLDs without vs. TLDs with magnet and 95 %-CI [−0.9 Gy; 0.2 Gy] and a mean dose difference of −0.1 Gy and 95 %-CI [−0.7 Gy; 0.3 Gy] for the comparison of the film measurements without and with magnet. Negative values represent a higher dose with magnet than without. Wilcoxon signed rank test showed significant differences with $p < 0.001$ in both cases.

In Fig. 5d there is no deviation to be seen in the direct comparison between the TPS calculation without and with magnet: The mean difference was 0.0 Gy with a 95 %-CI [−0.1 Gy; 0.2 Gy]. Negative values represent a higher dose with magnet than without. In this case Wilcoxon signed rank test showed no significant differences with $p = 0.052$.

Analysis of the actual clinical workflow showed a mean dose difference between the TLD measurements with magnet and the TPS calculations without magnet of −0.3 Gy and a 95 %-CI of [−1.4 Gy; 0.5 Gy]. The same scenario for film dosimetry showed a mean dose difference of -0.3 Gy and a 95 %-CI of [−1.3 Gy; 0.3 Gy]. Negative values represent a higher calculated dose, positive values a higher measured dose. Both boxplots are shown in Fig. 5e. Wilcoxon signed rank test resulted in a significant difference with $p < 0.001$ in both cases.

The results of an adapted workflow are shown in Fig. 5f. Dose differences for TLDs vs. TPS with magnet resulted in a mean dose difference of -0.3 Gy and a 95 %-CI of [-1.3 Gy; 0.5 Gy]. For films vs. TPS with magnet the mean dose difference was −0.3 Gy with a 95 %-CI [−1.2 Gy; 0.3 Gy]. Negative values represent a higher calculated dose, positive values a higher measured dose. Both showed significance differences with $p < 0.001$ in the Wilcoxon signed rank analysis.

For all treatment plans recalculated on the phantom, the maximum

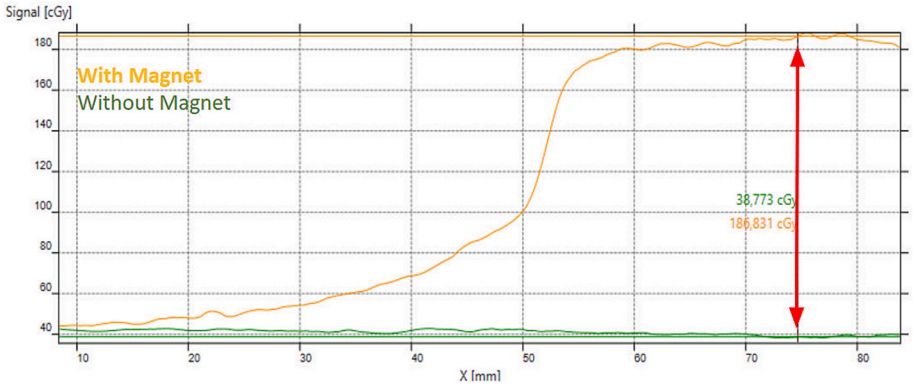


Fig. 4. Dose profiles of direct irradiation with magnet and without. The figure shows the dose profiles of the measured reference film without magnet (green) and measured film with magnet (yellow) on the RW3 phantom surface. Direct irradiation of the magnet results in a skin dose increased by a factor 5 below the magnet. Maximum dose difference is marked as red arrow.

Table 2
Results of the CIED-phantom study. Results from the different quantification scenarios. (-) means measurements or calculations without magnet and (+) with magnet.

Quantifications		Dose difference at mean with 95 %-CI – all in Gy
Deviations between measurement methods	TLDs(-) - Films(-)	−0.1 Gy [-0.6; 0.8]
Deviations between off-beam dosimetry and TPS	TLDs(-) - TPS(-)	−0.4 Gy [-1.5; 0.3]
	Films(-) - TPS(-)	−0.4 Gy [-1.4; 0.4]
Actual influence of the magnet on the dose to the CIED	TLDs(-) - TLDs(+)	−0.1 Gy [-0.9; 0.2]
	Films(-) - Films(+)	−0.1 Gy [-0.7; 0.3]
Influence of the virtual magnet on the calculated dose distribution	TPS(-) - TPS(+)	0.02 Gy [-0.1; 0.2]
Actual clinical workflow	TLD(+) - TPS(-)	−0.3 Gy [-1.4; 0.5]
	Film(+) - TPS(-)	−0.3 Gy [-1.3; 0.3]
Adapted clinical workflow	TLD(+) - TPS(+)	−0.3 Gy [-1.3; 0.5]
	Film(+) - TPS(+)	−0.3 Gy [-1.2; 0.3]

dose was recorded over all TLD ROI around the CIED. Calculated doses in the TLD ROIs ranged from 0.1 Gy to 9.0 Gy without magnet and 0.1 Gy to 8.0 Gy with magnet. TLD measurements resulted in doses of 0.2 Gy to 5.0 Gy without and 0.3 Gy to 5.2 Gy with magnet. Film measurements showed a range of 0.3 Gy to 5.6 Gy without and 0.2 Gy to 5.7 Gy with magnet at the TLD positions. According to the dose calculation in the TPS, a $D_{max} < 2.0$ Gy was achieved in 5 out of the 15 cases. In 10 cases the D_{max} was within 2.0 Gy to 10.0 Gy, and $D_{max} > 10.0$ Gy in none of the cases. Inclusion of the magnet in the dose calculation did not change the classification. Assuming no pacemaker dependence, this corresponds to a low risk classification in 5 and a medium risk classification in 10 cases as it is shown in Table 3. The low risk classification was confirmed by the film measurements with and without magnet and TLD measurements without magnet in all cases. In one case (Pat #5), TLD measurements with magnet on the surface resulted in a $D_{max} \geq 2.0$ Gy (2.0 Gy and 2.2 Gy in 2 out of 16 TLD respectively) in contrary to TPS calculations and film measurements, which might change the risk classification to medium in this case. According to measurements the placement of the magnet changed the classification from low to medium in 1 case (films, Pat #7) and 2 cases (TLDs, Pat #5 and #7) respectively. The medium risk classification by the TPS was changed to low according to film measurements in two cases without magnet and in one case with magnet and was confirmed in all but one of the cases by the TLD measurements. Taking all 30 treatments (15 deliveries with and 15 deliveries without magnet) into account, the risk classification by the TPS was correct in 87 %, too high in 10 % and potentially too low in 3 % of the treatments.

Discussion

The purpose of this study was to investigate if the magnet used for deactivation of ATA therapy has a clinically relevant influence on CIED dose in radiation therapy, to evaluate the inclusion of the magnet in the treatment planning process, and to evaluate the safety of risk classification based on TPS calculations for patients with esophageal or naso-oropharyngeal carcinoma.

As observed in the first simplified measurement setup, positioning of the magnet in the open beam resulted in a 20 % dose reduction in 3 to 5 cm depth below the magnet. At the surface, the dose increased by a factor of 5. While direct irradiation of the CIED is generally avoided in treatment planning, partial irradiation of the magnet by individual segments of a VMAT plan may occur, if the position of the magnet is not included in the treatment planning process. In cases where PTV is located near the CIED, the magnet should therefore be delineated in the treatment planning CT data. Thus, irradiation through the magnet can be avoided in the optimization of the treatment plan in order to prevent increased skin dose.

For the main investigation CT data of 15 patients previously treated for esophageal or naso-oropharyngeal carcinoma at our department were used for treatment planning with a prescription dose of 45.0 Gy and 70.0 Gy respectively. VMAT plans were optimized without inclusion of the magnet in the treatment planning process for each patient. All plans were transferred to the CT scan of an in-house developed thoracic phantom incorporating a CIED for dose calculation. The plans were recalculated with and without a magnet on the surface of the phantom. All plans were delivered to the phantom with and without magnet on the surface using TLD and films for dosimetry. Measured and calculated doses around the CIED were compared with and without magnet on the surface of the phantom to assess the influence of the magnet. Plans were classified into risk groups using calculated and measured maximum doses in the TLD positions as a surrogate for the maximum dose in the CIED.

Comparison of off-beam dosimetry methods showed minor differences between TLDs and film measurements with a mean dose difference of 0.1 Gy or 3 %. Due to the large sample size of 240 and outliers in the TLD measurements, even these small mean differences led to small p-values and statistically significant results. The outliers can be explained as follows: For the calibration process, the TLDs were positioned in the primary high energy beam. As shown in [13], the probability of a photoelectric effect in the TLD material is higher at low photon energies.

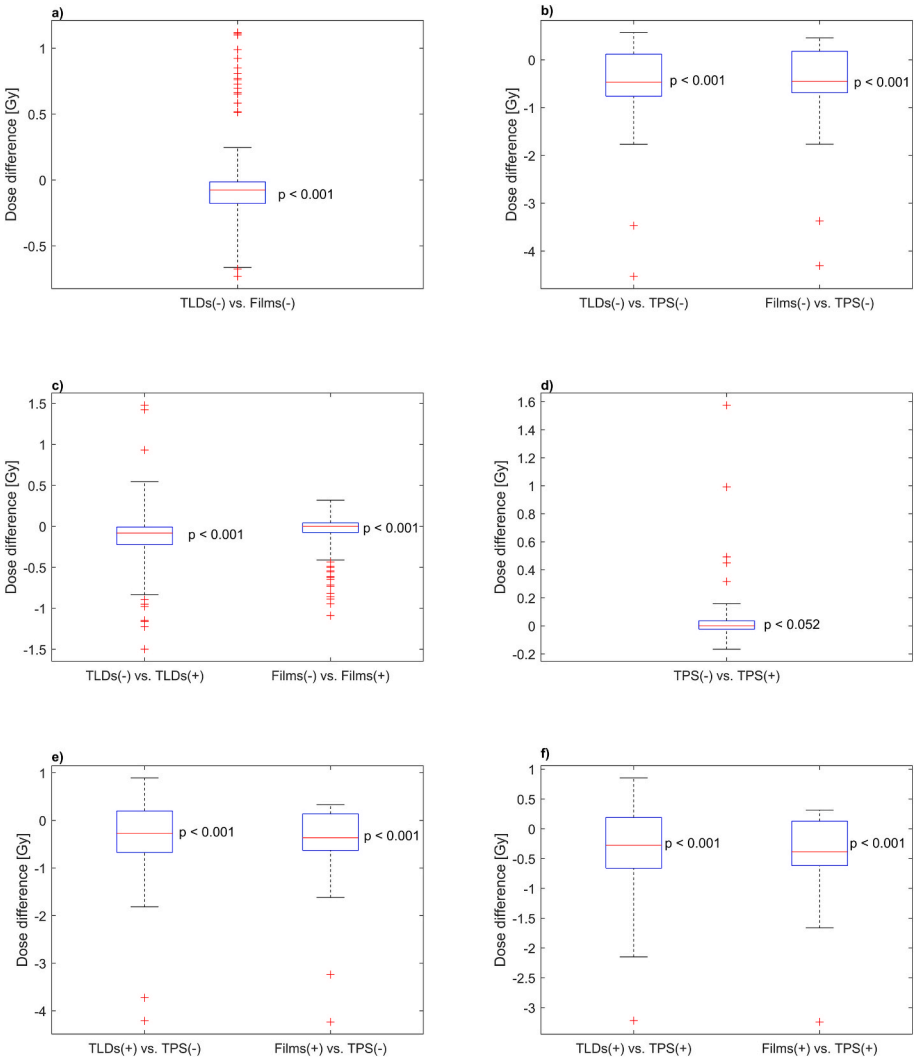


Fig. 5. Results of the different comparison scenarios. The Figure shows the results as boxplots. The red marker in the middle shows the median. Lower and upper edges of the boxplots are the 1st and 3rd quartiles. Extreme data points are shown by the black whiskers and characterized with up to 3 interquartile ranges. Outliers larger than 3 interquartile ranges are demonstrated with the red symbol "+". The p-value is shown in each figure. a) Quantification of deviations between measurement methods - Comparison of TLDs to films measurements, both without (-) magnet. b) Quantification of deviations between off-beam dosimetry and TPS - Comparison of measurements (TLD and films) to calculation, all without (-) magnet. c) Quantification of actual influence of the magnet on the dose to the CIED -Comparison of TLD measurements with magnet (+) to without magnet (-) and comparison of film measurements with magnet (+) to without (-). d) Quantification of the influence of the virtual magnet on the calculated dose distribution - Direct comparison of TPS calculations with (+) and without (-) magnet. e) Assessment of actual clinical workflow - Actual clinical workflow means comparison of TPS calculation without (-) magnet to TLD and film measurements with (+) magnet. f) Assessment of adapted clinical workflow - Adapted clinical workflow means comparison of TPS calculation with (+) magnet to TLD and film measurements with (+) magnet.

Table 3
Changes to the risk classifications based on the results. Risk classification for the 15 plans according to calculations and measurements of the dose in the TLD ROIs around the CIED assuming no pacemaker dependence. Calculations and measurements without magnet are labeled "-", with magnet "+".

Pat #	TPS-	TLD-	Film-	TPS+	TLD+	Film+
1–4	low	low	low	low	low	low
5	low	low	low	low	medium	low
6	medium	medium	low	medium	medium	low
7	medium	low	low	medium	medium	medium
8–15	medium	medium	medium	medium	medium	medium

This can lead to an overestimation of the dose in the out-of-field region of up to 12 %. It must also be taken into account, that new TLDs were used in this work, which had to be calibrated and stabilized first. This leads to further inaccuracies, that can be further reduced in future stabilization measurements.

The results showed a statistically significant but small influence of the magnet used for ATA deactivation on the dose to the CIED. Averaged over all measurements, the dose was increased by 0.1 Gy when the magnet was positioned at the surface of the patient. The increase was limited to 0.3 Gy according to the 95 % CI. Decreases of up to 0.9 Gy were observed. A decrease in dose to the CIED is clinically favourable, whereas an increase might lead to a classification into a higher risk group. According to film and TLD measurements, the placement of the magnet led to a classification into a higher risk group in 1 of the 15 cases, according to TLD measurements only in 1 additional case. Taking the uncertainties of films (2 %) and TLDs (9 %) into account, the change of classification based on TLDs only seems, however, questionable, especially because the maximum dose measured by the TLDs in this case was 2.2 Gy i.e. 9 % above the dose limit for a low risk classification.

Dose measurements in the off-beam region showed deviations to the dose calculations in the TPS irrespective of the use of a magnet for ATA

deactivation. Averaged over all TLD ROIs, the dose was overestimated by the TPS by 0.4 Gy and ranged from an overestimation of 1.5 Gy to an underestimation of 0.4 Gy in the case without magnet. When the magnet was positioned on the surface of the phantom, the dose was overestimated by 0.3 Gy on average and ranged from an overestimation of 1.4 Gy to an underestimation of 0.5 Gy. There was no effect of the inclusion of the magnet in the dose calculation. An overestimation of the CIED dose may lead to an erroneous classification into a higher, an underestimation into a lower risk group, which is clinically more relevant. When a maximum dose in the CIED of 1.5 Gy to 2.0 Gy is calculated by the TPS, measurements are therefore useful to avoid erroneous classification into the lower risk group.

Delana et al. [23] studied the out-of-field accuracy of four different treatment planning systems in the presence of a pacemaker in a slab phantom. They compared dose calculations in the TPS with TLD and metal oxide semiconductor field-effect transistor (MOSFET) measurements at 3 positions around the pacemaker for an unmodulated and a modulated static field and a left breast treatment with two modulated beams. For the highly modulated fields for an Elekta linear accelerator (LINAC) and the XVMC dose calculation in Monaco they found that the TPS overestimates the out-of-field dose by around 40 % on average and up to nearly 100 % at 10 cm from the field edge and doses below 0.1 Gy. This is in line with our findings of an average overestimation of the dose by 20 % for more complex VMAT treatments. In the publication of Delana et al. data are given, however, as average ± standard deviation, and no information is given on the 95 %-CI or the range of underestimation by the TPS to our understanding. Our results confirm the findings of Delana et al. for the combination of Monaco and Elekta LINACs, adding information for more complex VMAT treatments and the use of the magnet for ATA deactivation.

The evaluation of the classification into risk groups in our study showed, that despite the uncertainties in dose calculation, 87 % of the treatments were classified correctly into risk groups by the TPS. When no magnet was used for ATA deactivation, the dose calculation by the TPS led to a classification into medium risk instead of low, which is clinically of minor relevance, in 10 % of the treatments. An erroneous classification into a lower risk group was not observed in this case. When the magnet was placed on the surface of the phantom, the classification by the TPS might have erroneously resulted in a low risk according to TLD measurements in one case. Film measurements confirmed, however, the classification by the TPS. Due to measurement uncertainties and differences in film and TLD measurements, the classification remains ambiguous in this case. Risk classification by the TPS Monaco was safe in 97 % of the cases, even if a magnet was used for ATA deactivation and not included in the treatment planning process. An inclusion of the magnet in the treatment planning workflow is therefore not required for safe risk classification.

Limitations of the study are that minor measurement uncertainties must be included in the consideration of results, such as phantom alignment using lasers rather than CBCT to avoid radiation exposure of TLDs and films prior to the actual measurement process. Another uncertainty in CIED dose determination is our assumption of an iron magnet in the treatment planning process with a relative electron density of 6.6. The actual composition of the magnet is unknown and could lead to calculation uncertainties due to false density assumptions. Furthermore, the magnetic field of the magnet could not be taken into account in the TPS used for this study. To better understand and evaluate the influence of the magnetic field on CIED dose, future studies should be performed, using a planning system that integrates the magnetic field. In addition, it is important to note that the results are limited to the TPS Monaco. The accuracy of any treatment planning system depends on its beam model and should be evaluated on its own.

Conclusion

Our study showed a minor influence of the magnet on the CIED dose for VMAT irradiations of patients with esophageal or nasooropharyngeal carcinoma, where direct irradiation of the CIED is avoided at all cost. Risk classification by film and TLD measurements changed from low to medium in one out of 15 cases, when the magnet was positioned on the surface of the phantom. The dose calculation in the TPS overestimated the dose to the CIED by 0.4 Gy on average and the inclusion of the magnet in the TPS had no influence on calculated CIED dose and did not change the classification into risk groups. Risk classification by the TPS Monaco was safe in 97 % of the cases, even if a magnet was used for ATA deactivation and not included in the treatment planning process. Therefore, generally including the shape and the density of the magnet in the treatment planning is not considered necessary for safe risk classification. If the CIED is located close to the PTV, delineation of the magnet in the treatment planning CT data is, however, reasonable, to prevent unwanted partial irradiation of the magnet and thus an undesirable high skin dose.

CRediT authorship contribution statement

Larissa Blümlein: Writing – original draft, Visualization, Methodology, Investigation, Formal analysis, Data curation, Conceptualization. **Oliver Kölbl:** Writing – review & editing, Supervision. **Ralf Ringler:** Writing – review & editing, Supervision. **Barbara Dobler:** Writing – review & editing, Supervision, Funding acquisition, Conceptualization.

Declaration of competing interest

The authors declare that they have no known competing financial interests or personal relationships that could have appeared to influence the work reported in this paper.

Acknowledgments

This work was supported by the Bavarian State Ministry of Environment and Consumer Protection (StUMV) and the Bavarian Academic Forum (BayWISS). We would like to thank Dr. Harald Ostermeier from the hospital Barmherzige Brüder Regensburg for his support in the introduction of TLD measurements.

References

[1] Gauter-Fleckenstein B, Israel CW, Dorenkamp M, Dunst J, Roser M, Schimpf R, et al. DEGRO/DGK guideline for radiotherapy in patients with cardiac implantable electronic devices. Strahlenther Onkol 2015;191(5):393–404. https://doi.org/10.1007/s00066-015-0817-3.

[2] Markewitz A. Jahresbericht 2020 des Deutschen Herzschrittmacher und Defibrillator-Registers-Teil 2: Implantierbare Kardioverter-Defibrillatoren (ICD) 2022. Doi: 10.1007/s00399-022-00894-4.

[3] Markewitz A. Jahresbericht 2020 des Deutschen Herzschrittmacher und Defibrillator-Registers-Teil 1: Herzschrittmacher 2022. Doi: 10.1007/s00399-022-00893-5.

[4] Miften M, Mihailidis D, Kry SF, Reft C, Esquivel C, Farr J, et al. Management of radiotherapy patients with implanted cardiac pacemakers and defibrillators: a report of the AAPM TG-203†. Med Phys 2019;46(12):e757–88. https://doi.org/10.1002/MP.13838.

[5] Hurkmans CW, Knegjens JL, Oei BS, Maas AJJ, Uiterwaal GJ, van der Borden AJ, et al. Management of radiation oncology patients with a pacemaker or ICD: a new comprehensive practical guideline in The Netherlands. Dutch society of radiotherapy and oncology (NVRO). Radiat Oncol 2012;7:198. https://doi.org/10.1186/1748-717X-7-198.

[6] Mille MM, Jung JW, Lee C, Kuzmin GA, Lee C. Comparison of normal tissue dose calculation methods for epidemiological studies of radiotherapy patients. J Radiol Prot 2018;38(2):775–92. https://doi.org/10.1088/1361-6498/aabd4f.

[7] Fradley MG, Lefebvre B, Carver J, Cheung JW, Feigenberg SJ, Lampert R, et al. How to manage patients with cardiac implantable electronic devices undergoing radiation therapy. JACC CardioOncol 2021;3(3):447–51. https://doi.org/10.1016/j.jaccao.2021.08.005.

[8] Jacob S, Panaich SS, Maheshwari R, Haddad JW, Padanilam BJ, John SK. Clinical applications of magnets on cardiac rhythm management devices. Europace 2011;13(9):1222–30. https://doi.org/10.1093/europace/eur137.

[9] Krieger H. Grundlagen der Strahlungsphysik und des Strahlenschutzes. sixth ed. Berlin: Springer Spektrum; 2019.

[10] Kry SF, Bednarz B, Howell RM, Dauer L, Followill D, Klein E, et al. AAPM TG 158: Measurement and calculation of doses outside the treated volume from external-beam radiation therapy. Med Phys 2017;44(10):e391–429. https://doi.org/10.1002/mp.12462.
[11] RadPro International GmbH. Thermoluminescent Detectors. [February 17, 2025]; Available from: https://www.radpro-int.com/tld-1/tld-material/.
[12] Hauri P, Schneider U. Whole-body dose and energy measurements in radiotherapy by a combination of LiF:Mg,Cu,P and LiF:Mg. Ti. Z Med Phys 2018;28(2):96–109. https://doi.org/10.1016/j.zemedi.2017.07.002.
[13] Kry SF, Alvarez P, Cygler JE, DeWerd LA, Howell RM, Meeks S, et al. AAPM TG 191: clinical use of luminescent dosimeters: TLDs and OSLDs. Med Phys 2020;47(2):e19–51. https://doi.org/10.1002/mp.13839.
[14] Ashland Inc. GAFCHROMIC Dosimetry Media, Type EBT-3. Manual. [April 23, 2023]; Available from: http://www.gafchromic.com/gafchromic-film/radiotherapy-films/EBT/index.asp.
[15] Menegotti L, Delana A, Martignano A. Radiochromic film dosimetry with flatbed scanners: a fast and accurate method for dose calibration and uniformity correction with single film exposure. Med Phys 2008;35(7):3078–85. https://doi.org/10.1118/1.2936334.
[16] Maerz M, Koelbl O, Dobler B. Influence of metallic dental implants and metal artefacts on dose calculation accuracy. Strahlenther Onkol 2015;191(3):234–41. https://doi.org/10.1007/s00066-014-0774-2.
[17] Beveridge S, Alves A, Hussein M, Clark CH, Jornet N, Viegas CCB, et al. An international film dosimetry intercomparison to establish a multi-center audit framework. Med Phys 2024;51(12):9071–87.
[18] Sorriaux J, Kacperek A, Rossomme S, Lee JA, Bertrand D, Vynckier S, et al. Evaluation of Gafchromic® EBT3 films characteristics in therapy photon, electron and proton beams. Phys Med 2013;29(6):599–606. https://doi.org/10.1016/j.ejmp.2012.10.001.
[19] Cohen J. Statistical Power Analysis for the Behavioral Sciences. 2nd ed.
[20] Faul F, Erdfelder E, Buchner A, Lang A-G. G*Power 3: a flexible statistical power analysis program for the social, behavioural, and biomedical sciences. Behav Res Methods 2007. https://doi.org/10.3758/bf03193146.
[21] Faul F, Erdfelder E, Buchner A, Lang A-G. Statistical power analyses using G*Power 3.1: Tests for correlation and regression analyses. Behav Res Methods 2009;41(4):1149–60. https://doi.org/10.3758/BRM.41.4.1149.
[22] Wang FK. Confidence interval for the mean of non-normal data. Qual Reliab Eng 2001;17(4):257–67. https://doi.org/10.1002/qre.400.
[23] Delana A, Barbareschi A, Consorti R, Daniela FM. Dose calculation accuracy in proximity of a pacemaker: a multicenter study with threecommercial treatment planning systems. Physica medica 2020;80:201–8. https://doi.org/10.1016/j.ejmp.2020.10.015.